



Full Length Article

N-doped graphene sheets induced high electrochemical activity in carbon film

Liangliang Huang^{a,b}, Yuanyuan Cao^a, Dongfeng Diao^{a,*}^a Institute of Nanosurface Science and Engineering (INSE), Guangdong Provincial Key Laboratory of Micro/Nano Optomechatronics Engineering, Shenzhen University, Shenzhen 518060, China^b Key Laboratory of Optoelectronic Devices and Systems of Ministry of Education and Guangdong Province, College of Optoelectronic Engineering, Shenzhen University, Shenzhen 518060, China

ARTICLE INFO

Keywords:

Carbon film
N-doped graphene sheets
Electrochemical activity
Biosensor

ABSTRACT

In this study, we prepared a carbon film with clearly shaped N-doped graphene sheets by electron cyclotron resonance (ECR) plasma sputtering under low-energy electron irradiation. We found the N-doped graphene sheets remarkably improved the electrochemical activity of carbon film. The charge-transfer resistance was decreased from 21.62 Ω cm² to 1.37 Ω cm², and the redox peak separation was reduced to a low value of 65.4 mV in Fe(CN)₆^{4-/3-} redox system. The high electrochemical activity of N-doped graphene sheets embedded carbon (N-GSEC) films was ascribed to the formation of smaller sized N-doped graphene sheets. The smaller sized N-doped graphene sheets with high electronic density of states produced abundant edge defects, which served as active sites, facilitated the adsorption of Fe(CN)₆^{4-/3-} on film surface and enhanced the electron transfer. In detecting DNA base of adenine, the N-GSEC film showed a low oxidation potential and high sensitivity. These results demonstrate the N-GSEC film is a promising candidate material for construction sensitivity electrochemical biosensor.

1. Introduction

Amorphous carbon (a-C) films have attracted much attention in recent years as analysis electrode materials for application in biosensor because of their advantageous electrochemical properties [1,2]. Compared with the classical glassy carbon electrode (GCE), a-C films exhibit a wider potential window and lower background current [3,4]. In order to overcome the disadvantage of a-C, the low electrochemical activity, many efforts have been devoted to improve the film structure [5]. Niwa et al. [6,7] prepared a carbon film with nanocrystalline graphite structure by ion irradiation electron cyclotron resonance (ECR) plasma sputtering. This film exhibited wider potential window and higher electrochemical activity than the classical GCE, and could be applied in detecting single-nucleotide polymorphisms [8] and 5-Methylcytosine [9]. Diao et al. [10] prepared a carbon film called graphene sheets embedded carbon (GSEC) film by low-energy electron irradiation ECR plasma sputtering. The nanosized graphene sheets highly enhanced the electrochemical activity of carbon film because the vertical graphene sheets offered fast electron transport path and more reactive sites.

Besides forming nanocrystalline structure, heteroatom doping is another effective method to improve the electrochemical activity of a-C

films. Among of them, the nitrogen atom is the most widely researched since the similar atomic size to carbon [11]. Cao et al. [12] realized the application of amorphous carbon as metal free electrocatalyst in oxygen reduction reaction by N-doping. The N-doping could decrease the electrical resistivity of tetrahedral a-C films [13], and improve the electrocatalytic activity and reactivity [14].

Therefore, by taking advantages of N-doping and forming nanocrystalline structure, the electrochemical activity of a-C films should be further improved. Especially in the GSEC films, there contained many nanosized graphene sheets. The electrochemical property of N-doped graphene is much better than pure graphene since with higher electronic density of states [15–19]. However, the N-doped graphene sheet is not easy to form in carbon film. Although some methods have been tried to prepare N-doped graphene in carbon film [14], there has no report that successful prepared clear shaped N-doped graphene sheets in carbon film until now.

In this article, we tried to prepare a carbon film with clearly shaped N-doped graphene sheets by N-doping in GSEC film, and investigated the effects of N-doping on the structure and electrochemical properties of GSEC film. The N-GSEC films structure were characterized by using transmission electron microscopy (TEM), atomic force microscopy

* Corresponding author.

E-mail address: dfdiao@szu.edu.cn (D. Diao).

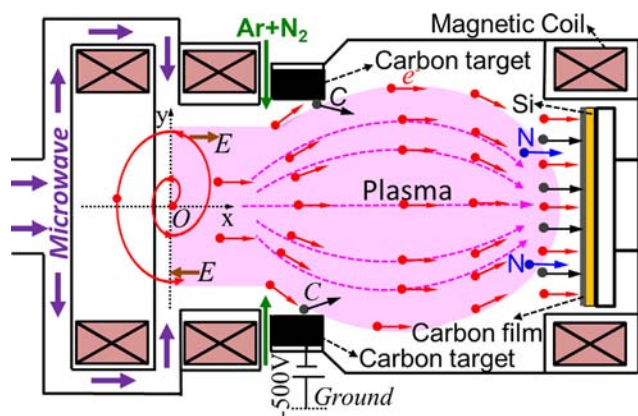


Fig. 1. A schematic illustration of ECR low-energy electron irradiation forming N-GSEC.

(AFM), Scanning Electron Microscope (SEM), Raman spectra and X-ray photoelectron spectroscopy (XPS). The electrochemical properties were also investigated by electrochemical impedance spectroscopy (EIS) and cyclic voltammetry (CV). At last, the N-GSEC films electrodes were used to detect DNA base of adenine with differential pulse voltammetry (DPV).

2. Experimental

2.1. Film preparation

All carbon films were deposited on boron-doped silicon wafer (100) substrate by ECR low-energy electron irradiation as showed in Fig. 1. The chamber was firstly pumped to a background pressure of 8.0×10^{-5} Pa, and then, the mixture gas of argon and N_2 were introduced as working gas and kept a pressure of 4.00×10^{-4} Pa. The ratios of N_2 were 0%, 8%, 15%, 25% and 40%, the corresponding films were named as CN0, CN1, CN2, CN3 and CN4, respectively. However, the sample CN4 could not form normally. The substrate bias voltage was +80 V. The microwave power and carbon target bias voltage were 500 W and -500 V, respectively. The thicknesses of these films were about 60 nm.

2.2. Film characterization

The nanostructures of film were characterized with high-resolution TEM (Titan3 Themis G2) at an electron acceleration voltage of 300 kV. The surface morphologies and roughness were measured by Dimension Edge AFM with a BRUKER SCANASYST-AIR tip at room temperature. The scanning rate is 1 Hz with 512×512 pixels. The SEM (FEI Scios) was also used to characterize the surface morphologies of carbon films.

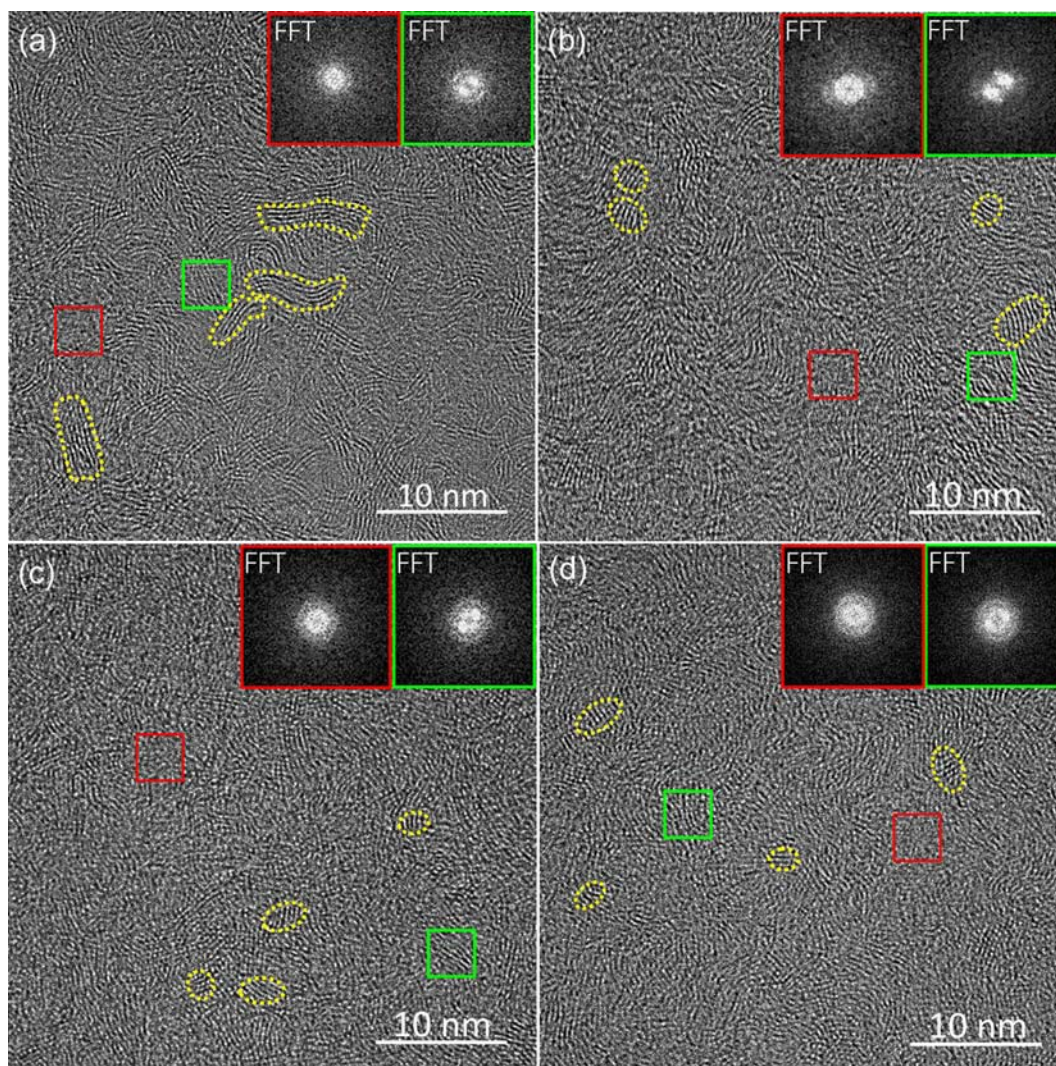


Fig. 2. The TEM images of carbon films: (a) CN0; (b) CN1; (c) CN2 and (d) CN3, and inserted FFT images corresponding to green (multilayer graphene sheets) and red (amorphous) squares regions, respectively.

The XPS (ThermoScientific ESCALAB 250Xi) and Raman spectroscopy (HORIBA, LabRAM HR Evolution) were used to determine the elemental composition and the quantity of chemical bonds.

2.3. Electrochemical measurements

Electrochemical experiments were carried out in a standard three-electrode cell with an electrochemistry workstation of Gamry Reference 600+. The carbon film with an area about 0.2 cm² was served as working electrode. A Pt wire and Ag/AgCl were used as counter electrode and reference electrode respectively. The EIS was measured from 0.1 Hz to 100 kHz in two redox system. The AC signal amplitude was 10 mV. In 5 mM Fe(CN)₆^{4-/-3-} and 1 M KCl solution, the DC was set at 0.26 V vs. Ag/AgCl. In 5 mM Ru(NH₃)₆^{2+/-3+} and 1 M KCl solution, the DC was set at -0.15 V vs. Ag/AgCl. The CVs in 1 mM Fe(CN)₆^{4-/-3-} and 1 M KCl were also measured. The DPV of Adenine (A) with different concentration in 0.1 PBS (pH = 7.0) were tested. The step size and pulse size were 5 mV and 25 mV, respectively. All electrochemical measurements were repeated at least 3 times with different electrodes at room temperature.

3. Results and discussion

3.1. Chemical and surface structures

The effects of N-doping on the nanostructure of GSEC films were firstly characterized with TEM. As shown in Fig. 2, nanosized graphene sheets have been formed in four samples. The fast Fourier transformation (FFT) showed two white light spots in the green marked regions, which confirmed the formation of multilayer graphene. In the red square regions, FFT showed no pattern corresponding to amorphous structure. It suggests the graphene sheets are also formed under N₂ and Ar mixture gas. Compared with pure carbon film sample, the size of N-doped graphene sheets were obviously decreased, especially in the length of graphene sheets. However, compared with ECR ion irradiation [14], more clearly shaped N-doped graphene sheets were obtained in ECR electron irradiation under N₂ and Ar mixture gas. As shown in Fig. 3, the surface morphologies of these four carbon were almost the same based on AFM characterization. The surface roughness of carbon films were slightly decreased after being doped with nitrogen as shown in Table 1. The decreased roughness should be related with the reduced size of N-doped graphene sheets. The surface morphologies characterized with SEM, it showed the surface of these carbon films are very smooth as shown in Fig. S1. It suggested the carbon films structures are uniform.

The Raman spectra were measured for studying the bonding configuration of carbon films as shown in Fig. 4(a). All samples presented separable D and G peak around 1355 cm⁻¹ and 1597 cm⁻¹, respectively. The D peak intensity of N-doped GSEC was much lower than that of GSEC. It means the film structure ordering is decreased by N-doping since the D peak corresponding to the long range ordered structures with sp² hybridization [2]. This is consistent with the decreasing of I_D/I_G, which relates to clustering and ordering of sp² phase [20,21] as shown in Table 1. Based on the references [22,23], the average size of graphene nanocrystalline were calculated, the values of CN0, CN1, CN2 and CN3 were 1.45 nm, 1.29 nm, 1.31 nm and 1.30 nm, respectively. Therefore, it can be concluded that N-doping inhibits the clustering of sp² phase and results in decreasing of structure ordering and nanocrystalline size.

To further gain insight into the chemical composition and bonding of N-GSEC films, XPS was carried out as shown in Fig. 4(b) and Table 1. The O/C atomic ratio decreased from 3.33% to 3.10%, and sp² content decreased from 84.34% to 78.90% when the nitrogen partial pressure increased from 0% (sample CN0) to 8% (sample CN1). With the further increasing of N₂ partial pressure, both the O/C and nitrogen atom contents increased slightly, but the sp² content decreased a little. These

results suggest that N-doped graphene sheets are produced, but the N-doping restrains the formation of sp² phase. Meanwhile, the doping nitrogen content is very low and almost remains stable although the N₂ partial pressure increases significantly.

The high-resolution XPS N 1s spectra were fitted and decomposed into three peaks of pyridinic N, pyrrolic N and graphitic N at the binding energies of 398.4 eV, 399.9 eV and 401.2 eV [15], respectively. As shown in Fig. 5, N atoms bonded with C atoms mainly by pyridinic N and graphitic N in N-GSEC films. With the increasing of nitrogen contents, the ratio of graphitic N increased, and the pyridinic N decreased. Both the pyridinic N and graphitic N are helpful to improve the electrochemical properties of carbon materials [14,15]. However, the pyridinic N could only exist at the edge regions of six-membered rings and thought to be an estimative indicator of the discontinuity the graphite clusters [24]. Thus, the further growth of graphene will be inhibited when the pyridinic N is formed in graphene during the ECR deposition under electron irradiation. Therefore, the existence of pyridinic N may be the reason that results in the decreasing of graphene sheets size.

3.2. Electrochemical performance

To quantify the electronic and ionic conductivities, the EIS were measured in two redox system of Ru(NH₃)₆^{2+/-3+} and Fe(CN)₆^{4-/-3-}. As shown in Fig. 6, only one time-constant was observed in both two redox system. At high-frequency range, the Nyquist plots showed a semi-circle. A straight line with a 45° slope at low-frequency range indicates the response is dominated by diffusion process. The EIS data was fitted with Randles circuit (R_s(CPE_{ct}W)) [25], the results showed in Table 2 and Table S1. The R_s, CPE and W_d represent the solution resistance, Constant Phase Element and Warburg impedance, respectively. The charge-transfer resistance R_{ct} is composed of two parts: one is the electron transport resistance through the film; the other is electron transfer resistance between film surface and redox species [26]. In the outer-sphere redox system of Ru(NH₃)₆^{2+/-3+}, which not affected by the surface state of electrode [27], the R_{ct} values of four samples were almost the same. However, in the inner-sphere redox system of Fe(CN)₆^{4-/-3-}, the R_{ct} was reduced from 21.62 Ω cm² to 1.37 Ω cm². The kinetics of inner-sphere redox system is strongly influenced by the surface chemistry and electronic properties [28,29]. This suggests that N-doping has no obviously influence on the electron transport resistance, but decreases the electron transfer resistance significantly. The apparent heterogeneous rate constant (K⁰) [30] were calculated according to the value of charge-transfer resistance as shown in Table 2. It showed the K⁰ in N-GSEC was much lower than that in GSEC film. It proves that N-doping sharply improves the K⁰, and the kinetics of GSEC film in the inner-sphere redox system is extremely sensitive to N-doping.

The CV in Fe(CN)₆^{4-/-3-} were also measured to characterize the effects of N-doping on the electrochemical activity of GSEC films as shown in Fig. 7(a). The N-doping induced the peak separation (ΔE_p) decreased from 71.6 mV to 65.4 mV as listed in Table 2. The value of 65.4 mV is very close to the theoretical value (59 mV) of Nernstian one-electron reaction [31], and much lower than many other nanocarbon materials electrode, such as graphene [32], N-doped carbon nanofibers [33] and carbon nanowalls [34] et al. It indicates that N-doping makes the GSEC film get excellent electron transfer kinetics property.

The CVs with different scanning rate were further measured as shown in Fig. S2, and a linear relation between the logarithm of anodic peak current and logarithm of scanning rate were obtained as depicted in Fig. S3. The slope of four film electrodes are all about 0.49, which extremely close to the theoretical value of 0.5. It indicates the surface of four carbon films are all under diffusion-control in Fe(CN)₆^{4-/-3-} redox system. Meanwhile, as shown in Fig. 7(b), the electroactive surface area were estimated according to the Randles-Sevcik equation [31]. The values of CN0, CN1, CN2 and CN3 are 0.173 cm², 0.197 cm², 0.201 cm², 0.202 cm², respectively. It indicates N-doping effectively increases the

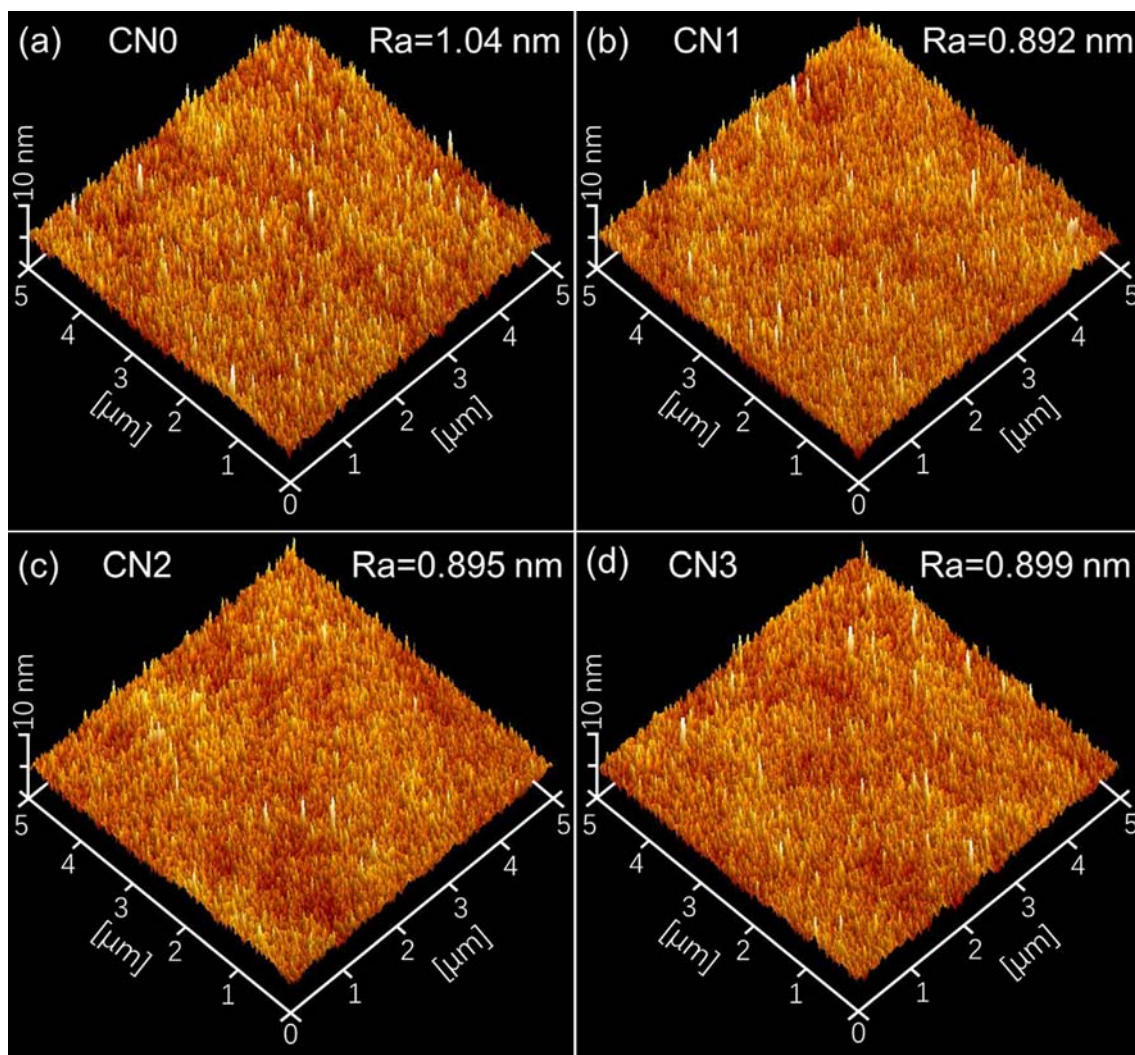


Fig. 3. The AFM images of carbon films: (a) CN0, (b) CN1, (c) CN2 and (d) CN3.

electroactive surface area. This explained the reason that the peak currents of N-GSEC films were higher than GSEC films in Fig. 7(a).

Based on the former structure analysis, it can be concluded that N-doping results in the decreasing of structure ordering and the forming of smaller sized N-doped graphene sheets since the pyridinic N inhibits the clustering of sp^2 phase as shown in Fig. 8(a). The formation of smaller sized N-doped graphene sheets produced more edge defects. As with higher local electronic density of states [5,32,35], these edge defects could serve as reactive sites and promoted electron transfer. For the inner-sphere redox system, the species should adsorb on the surface of electrode firstly before electron transferring (electrochemical reaction) [5]. The abundant edge defects at the surface of N-GSEC offered active sites for the adsorption of $Fe(CN)_6^{4-/3-}$ as shown in Fig. 8(b), and facilitated electron transfer at the interface. Therefore, the

formation of smaller sized graphene sheet is one important reason that causes high electrochemical activity of N-GSEC films. The other reason may be the N-doping itself increased the electronic density of states. The N-doping induced the Fermi level of graphene shifted toward into the conduction band since the nitrogen contained five valence electrons [19], and resulted in local electronic density of states near the Fermi level increasing [36]. Thus, the electron could be more easy be transferred between the N-GSEC film and redox species, and resulted in better electrochemical activity of N-GSEC in inner-sphere redox system. In addition, the pyridinic N could excite the adjacent carbon atom in graphene [15], and so, both the pyridinic N and carbon could be served as reaction active sites [37] facilitated electron transfer as shown in Fig. 8(b). For the outer-sphere redox system, N-doping exhibited no obvious influence on the electron transport resistance of GSEC. This

Table 1

The surface characterization data of carbon films with AFM, Raman and XPS.

	Ra (nm)	I_D/I_G	nanocrystalline size (nm)	$sp^2/(sp^2 + sp^3)\%$	O/C (%)	N (at.%)	N 1s (at%)		
							Pyridinic N	Pyrrlic N	Graphitic N
CN0	1.040	1.32	1.45	84.34	3.33	—	—	—	—
CN1	0.892	1.03	1.29	78.90	3.10	3.44	43.46	10.44	46.10
CN2	0.895	1.07	1.31	77.34	3.12	4.55	38.40	9.19	52.41
CN3	0.899	1.04	1.30	76.34	3.15	4.70	37.89	7.37	54.73

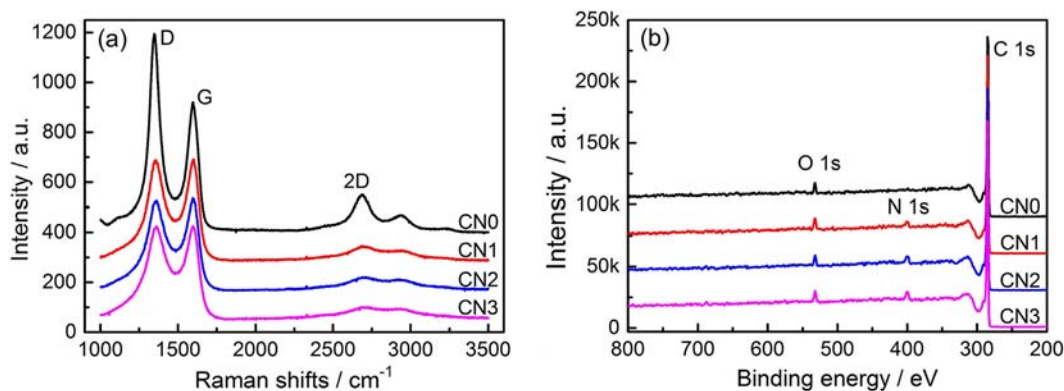


Fig. 4. Raman spectra (a) and XPS spectra (b) of carbon films.

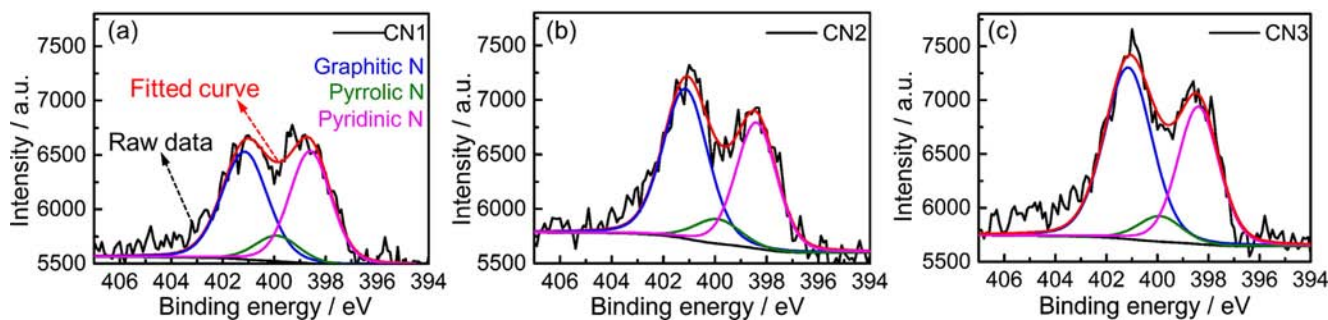


Fig. 5. High-resolution decomposition N 1s XPS spectra of N-doped carbon films: (a) CN1; (b) CN2 and (c) CN3.

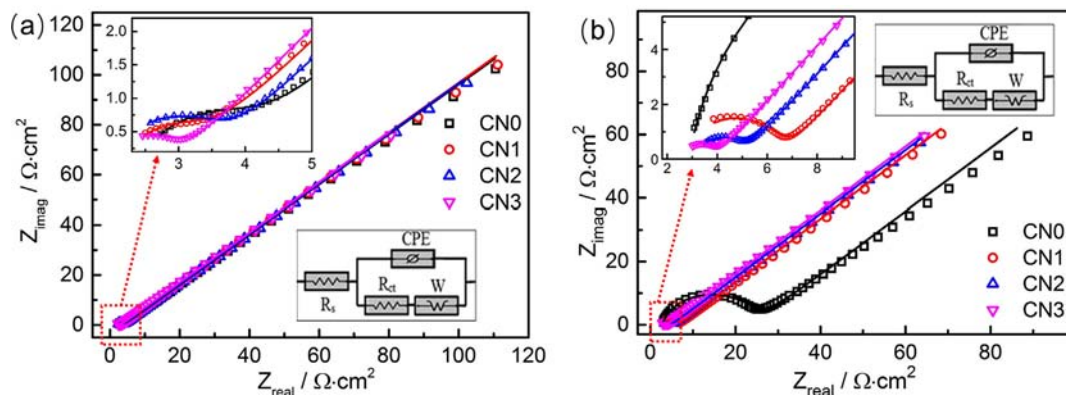


Fig. 6. Nyquist plots of carbon film electrodes obtained from EIS measurements in two redox system: (a) 5 mM $\text{Ru}(\text{NH}_3)_6^{2+/3+}$ in 1 M KCl; (b) 5 mM $\text{Fe}(\text{CN})_6^{4-/3-}$ in 1 M KCl (The inset is the equivalent circuit).

Table 2

The fitted results of EIS in 5 mM $\text{Fe}(\text{CN})_6^{4-/3-}$ and 1 M KCl, and the ΔE_p of cyclic voltammograms in 1 mM $\text{Fe}(\text{CN})_6^{4-/3-}$ and 1 M KCl with a scanning rate of 100 mV/s.

	$R_s / \Omega \text{ cm}^2$	$C_{dl} / \mu\text{F cm}^{-2}$	$W_d / 10^{-3} \Omega^{-1} \text{ s}^{1/2}$	$R_{ct} / \Omega \text{ cm}^2$	$K^0 / 10^{-2} \text{ cm s}^{-1}$	$\Delta E_p / \text{mV Fe}(\text{CN})_6^{4-/3-}$
CN0	2.37	6.70	22.67	21.62	0.25	71.6
CN1	2.46	11.8	13.94	3.63	1.47	67.9
CN2	2.78	18.71	12.07	1.88	2.83	65.9
CN3	2.60	25.75	13.03	1.37	3.89	65.4

maybe results from more amorphous formation is harmful to the electron transport in the film although N-doping increases local electronic density of states.

3.3. Application in detecting adenine

The DNA base of adenine was detected with two carbon films

electrode by DPV as shown in Fig. 9(a). The N-GSEC film obtained a much lower oxidation potential and higher oxidation peak current than GSEC film. It suggests that the N-GSEC film has better electrocatalytic activity for the oxidation of adenine. Then, the N-GSEC film electrodes were used to determine the adenine with different concentration as shown in Fig. 9(b). The oxidation peak current versus concentration of adenine displayed two different linear response at low and high

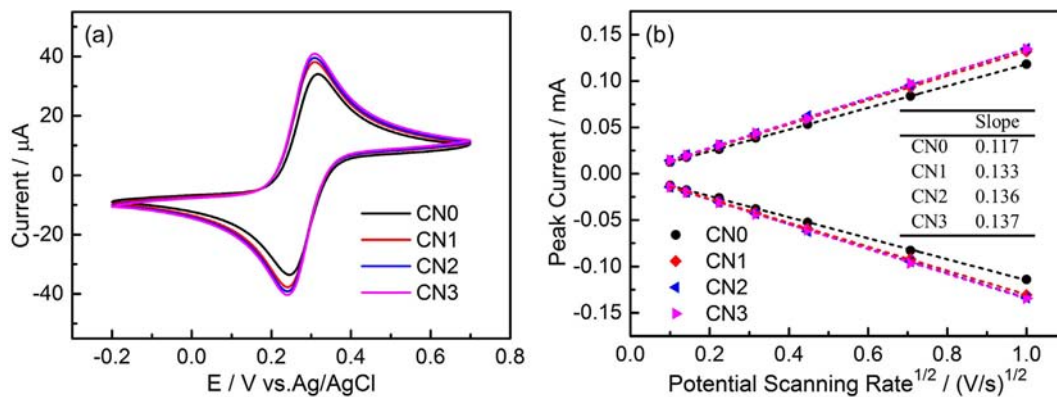


Fig. 7. (a) Cyclic voltammograms of carbon films in 1 mM $\text{Fe}(\text{CN})_6^{4-/3-}$ and 1 M KCl with a scanning rate of 100 mV/s; (b) Plot of peak current vs scan rate, insert table the slope of oxidation peak.

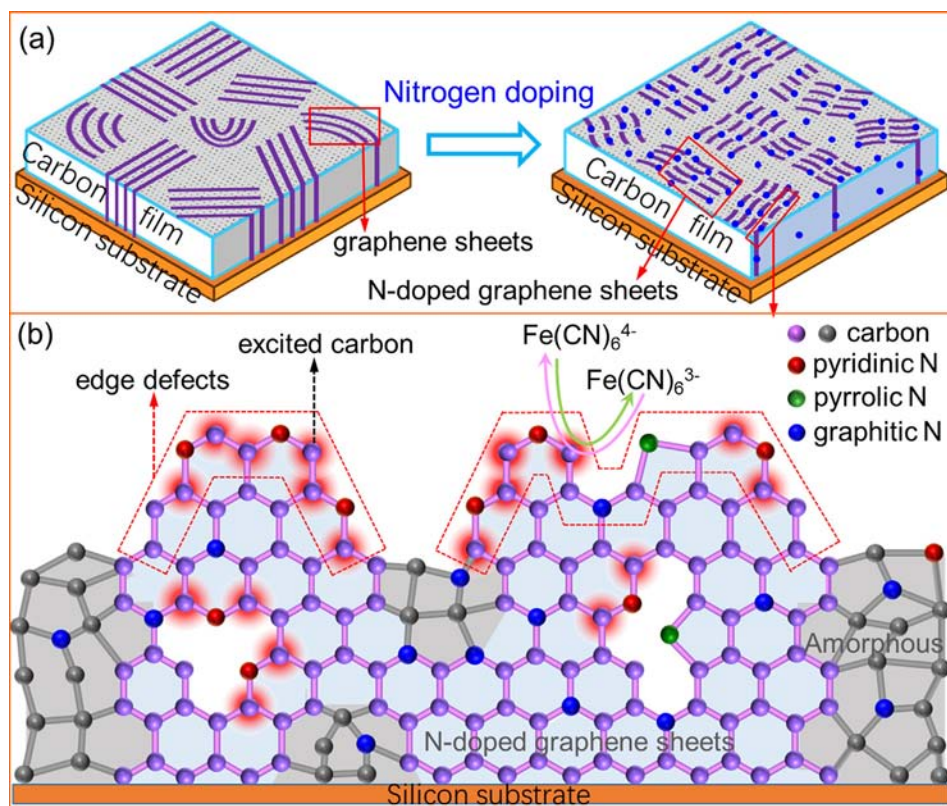


Fig. 8. Microstructures schematic of carbon film: (a) N-doping induced the formation of smaller sized N-doped graphene sheets in GSEC film; (b) Smaller sized graphene sheets produced more edge defects with high local electronic density of states. These edge defects served as active sites, facilitated the adsorption of $\text{Fe}(\text{CN})_6^{4-/3-}$ on film surface, and enhanced the electron transfer. In addition, the N atoms bonded with C atoms mainly by graphitic N and pyridinic N. N-doping increased the local electronic density of states near Fermi level, resulted in facilitating the electron transfer between $\text{Fe}(\text{CN})_6^{4-/3-}$ and carbon films, and improved the electrochemical activity. Especially the pyridinic N, which excited the adjacent carbon atoms to get better electron transfer kinetics.

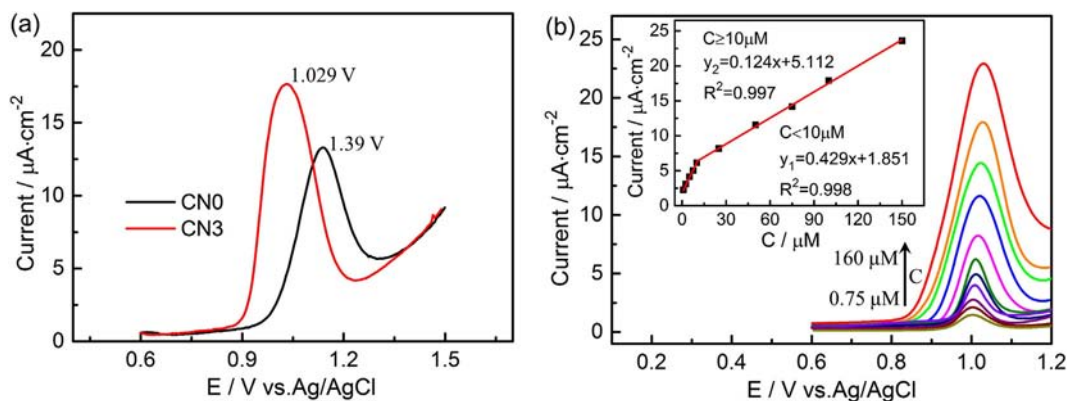


Fig. 9. (a) DPVs of carbon film electrodes in 0.1 mM adenine in PBS (pH = 7.0) and (b) DPVs of N-GSEC film (CN3) electrodes for detecting adenine with different concentrations in PBS (pH = 7.0).

concentration ranges. This phenomenon may be related with the formation of a monolayer of adsorbed adenine at the film surface and fits to Langmuir adsorption isotherm behavior [38,39]. The limit of detection of adenine is 0.5 μM . The linear detection range of adenine (signal-to-noise ≥ 3) is 0.75 μM ~ 160 μM . In order to achieve a better detection sensitivity, it's necessary to confirm the best N_2 partial pressure for preparing N-GSEC film in the future. This application demonstrates that the N-GSEC films have great potential in construction sensitivity biosensor since with excellent electrochemical activity.

4. Conclusions

A carbon film with clearly shaped N-doped graphene sheets was prepared by ECR low-energy electron irradiation. We found the N-doped graphene sheets remarkably improved the electrochemical activity of carbon film. The charge-transfer resistance was decreased from 21.62 Ωcm^2 to 1.37 Ωcm^2 and the redox peak separation was reduced to 65.4 mV in $\text{Fe}(\text{CN})_6^{4-/3-}$ redox system. Nitrogen atoms bonded with C atoms mainly by pyridinic N and graphitic N in N-GSEC films. With the increasing of nitrogen content, the ratio of graphitic N content gradually increased but the pyridinic N decreased. The N-doping inhibited the clustering of sp^2 phase, resulted in the decreasing of structure ordering, surface roughness and the size of graphene sheets. The formation of smaller sized N-doped graphene sheets was the key that induced the high electrochemical activity of N-GSEC films. The N-doped graphene sheets with high local electronic density of states produced abundant edge defects, which served as active sites, facilitated the adsorption of $\text{Fe}(\text{CN})_6^{4-/3-}$ on film surface and enhanced the interface electron transfer. In the application of detecting adenine, N-GSEC films decreased the oxidation potential of adenine significantly, and showed high sensitivity. This N-GSEC film exhibited great potential to be a sensitivity electrochemical biosensor in detecting biomolecules.

Acknowledgements

The authors acknowledge the financial support from National Nature Science Foundation of China (Grant NO. 51575359), China Postdoctoral Science Foundation (Grant NO. 2018M633124) and Shenzhen Fundamental Research subject-layout project (Grant NO. JCYJ20160427105015701). The authors are also grateful to Dr. Meijie Yin, Electron Microscopy Center of Shenzhen University, for helping in characterization of carbon film nanostructures.

Appendix A. Supplementary material

Supplementary data to this article can be found online at <https://doi.org/10.1016/j.apsusc.2018.11.075>.

References

- R.L. McCreery, Advanced carbon electrode materials for molecular electrochemistry, *Chem. Rev.* 108 (2008) 2646–2687.
- T. Palomäki, N. Wester, L.-S. Johansson, M. Laitinen, H. Jiang, K. Arstila, T. Sajavaara, J.G. Han, J. Koskinen, T. Laurila, Characterization and electrochemical properties of oxygenated amorphous carbon (a-C) films, *Electrochim. Acta* 220 (2016) 137–145.
- J.B. Jia, D. Kato, R. Kurita, Y. Sato, K. Maruyama, K. Suzuki, S. Hirono, T. Ando, O. Niwa, Structure and electrochemical properties of carbon films prepared by a electron cyclotron resonance sputtering method, *Anal. Chem.* 79 (2007) 98–105.
- K. Zhou, P. Ke, X. Li, Y. Zou, A. Wang, Microstructure and electrochemical properties of nitrogen-doped DLC films deposited by PECVD technique, *Appl. Surf. Sci.* 329 (2015) 281–286.
- W. Zhang, S. Zhu, R. Luque, S. Han, L. Hu, G. Xu, Recent development of carbon electrode materials and their bioanalytical and environmental applications, *Chem. Soc. Rev.* 45 (2016) 715–752.
- T.Y. You, O. Niwa, M. Tomita, T. Ichino, S. Hirono, Electrochemical oxidation of alkylphenols on ECR-sputtered carbon film electrodes with flat sub-nanometer surfaces, *J. Electrochem. Soc.* 149 (2002) E479–E484.
- O. Niwa, J. Jia, Y. Sato, D. Kato, R. Kurita, K. Maruyama, K. Suzuki, S. Hirono, Electrochemical performance of angstrom level flat sputtered carbon film consisting of sp^2 and sp^3 mixed bonds, *J. Am. Chem. Soc.* 128 (2006) 7144–7145.
- D. Kato, N. Sekioka, A. Ueda, R. Kurita, S. Hirono, K. Suzuki, O. Niwa, Nanohybrid carbon film for electrochemical detection of SNPs without hybridization or labeling, *Angew. Chem.-Int. Ed.* 47 (2008) 6681–6684.
- D. Kato, N. Sekioka, A. Ueda, R. Kurita, S. Hirono, K. Suzuki, O. Niwa, A nano-carbon film electrode as a platform for exploring DNA methylation, *J. Am. Chem. Soc.* 130 (2008) 3716–3717.
- L. Huang, Y. Cao, D. Diao, Nanosized graphene sheets induced high electrochemical activity in pure carbon film, *Electrochim. Acta* 262 (2018) 173–181.
- H. Xu, L. Ma, Z. Jin, Nitrogen-doped graphene: synthesis, characterizations and energy applications, *J. Energy Chem.* 27 (2018) 146–160.
- L. Cao, Z. Lin, J. Huang, X. Yu, X. Wu, B. Zhang, Y. Zhan, F. Xie, W. Zhang, J. Chen, W. Xie, W. Mai, H. Meng, Nitrogen doped amorphous carbon as metal free electrocatalyst for oxygen reduction reaction, *Int. J. Hydro. Energy* 42 (2017) 876–885.
- X. Yang, L. Haubold, G. DeVivo, G.M. Swain, Electroanalytical performance of nitrogen-containing tetrahedral amorphous carbon thin-film electrodes, *Anal. Chem.* 84 (2012) 6240–6248.
- T. Kamata, D. Kato, S. Hirono, O. Niwa, Structure and electrochemical performance of nitrogen-doped carbon film formed by electron cyclotron resonance sputtering, *Anal. Chem.* 85 (2013) 9845–9851.
- D. Guo, R. Shibuya, C. Akiba, S. Saji, T. Kondo, J. Nakamura, Active sites of nitrogen-doped carbon materials for oxygen reduction reaction clarified using model catalysts, *Science* 351 (2016) 361–365.
- H.M. Jeong, J.W. Lee, W.H. Shin, Y.J. Choi, H.J. Shin, J.K. Kang, J.W. Choi, Nitrogen-doped graphene for high-performance ultracapacitors and the importance of nitrogen-doped sites at basal planes, *Nano Lett.* 11 (2011) 2472–2477.
- H. Miao, S. Li, Z. Wang, S. Sun, M. Kuang, Z. Liu, J. Yuan, Enhancing the pyridinic N content of nitrogen-doped graphene and improving its catalytic activity for oxygen reduction reaction, *Int. J. Hydro. Energy* 42 (2017) 28298–28308.
- R. Sharma, S. Khan, V. Goyal, V. Sharma, K.S. Sharma, Investigation on effect of boron and nitrogen substitution on electronic structure of graphene, *FlatChem* 1 (2017) 20–33.
- W. Yin, T.-T. Jia, X. Guo, X. Huang, Y.-F. Zhang, W.-K. Chen, Effects of N-doping concentration on graphene structures and properties, *Chem. Phys. Lett.* 581 (2013) 74–79.
- A.C. Ferrari, J. Robertson, Interpretation of Raman spectra of disordered and amorphous carbon, *Phys. Rev. B* 61 (2000) 14095–14107.
- D.G. McCulloch, S. Prawer, A. Hoffman, Structural investigation of xenon-ion-beam-irradiated glassy carbon, *Phys. Rev. B* 50 (1994) 5905–5917.
- L.G. Cançado, K. Takai, T. Enoki, M. Endo, Y.A. Kim, H. Mizusaki, N.L. Speziali, A. Jorio, M.A. Pimenta, Measuring the degree of stacking order in graphite by Raman spectroscopy, *Carbon* 46 (2008) 272–275.
- M.J. Matthews, M.A. Pimenta, G. Dresselhaus, M.S. Dresselhaus, M. Endo, Origin of dispersive effects of the Raman D band in carbon materials, *Phys. Rev. B* 59 (1999) R6585–R6588.
- J. Li, Y. Zhang, X. Zhang, J. Huang, J. Han, Z. Zhang, X. Han, P. Xu, B. Song, S. N dual-doped graphene-like carbon nanosheets as efficient oxygen reduction reaction electrocatalysts, *ACS Appl. Mater. Interface* 9 (2017) 398–405.
- W. Li, Z. Zhang, Y. Tang, H. Bian, T.W. Ng, W. Zhang, C.S. Lee, Graphene-nanowall-decorated carbon felt with excellent electrochemical activity toward $\text{VO}_2^+/\text{VO}_2$ couple for all vanadium redox flow battery, *Adv. Sci.* 3 (2016) 1500276.
- T. Palomäki, N. Wester, M.A. Caro, S. Sainio, V. Protopenova, J. Koskinen, T. Laurila, Electron transport determines the electrochemical properties of tetrahedral amorphous carbon (ta-C) thin films, *Electrochim. Acta* 225 (2017) 1–10.
- T.-C. Kuo, R.L. McCreery, Surface chemistry and electron-transfer kinetics of hydrogen-modified glassy carbon electrodes, *Anal. Chem.* 71 (1999) 1553–1560.
- Y. Tanaka, M. Furuta, K. Kuriyama, R. Kuwabara, Y. Katsuki, T. Kondo, A. Fujishima, K. Honda, Electrochemical properties of N-doped hydrogenated amorphous carbon films fabricated by plasma-enhanced chemical vapor deposition methods, *Electrochim. Acta* 56 (2011) 1172–1181.
- P.H. Chen, R.L. McCreery, Control of electron transfer kinetics at glassy carbon electrodes by specific surface modification, *Anal. Chem.* 68 (1996) 3958–3965.
- E. Luis, M. Boujtita, A. Gohier, A. Tailleux, S. Casimirius, M.A. Djouadi, A. Granier, P.Y. Tessier, Carbon nanowalls as material for electrochemical transducers, *Appl. Phys. Lett.* 95 (2009) 3049.
- A.J. Bard, L.R. Faulkner, *Electrochemical Methods: Fundamental and Applications*, 2nd ed., John Wiley and Sons, New York, 2001.
- A. Ambrosi, A. Bonanni, M. Pumera, Electrochemistry of folded graphene edges, *Nanoscale* 3 (2011) 2256–2260.
- D. Liu, X. Zhang, T. You, Electrochemical performance of electrospun free-standing nitrogen-doped carbon nanofibers and their application for glucose biosensing, *ACS Appl. Mater. Interface* 6 (2014) 6275–6280.
- K. Siuzdak, M. Ficek, M. Sobaszek, J. Ryl, M. Gnyba, P. Niedziałkowski, N. Malinowska, J. Karczewski, R. Bogdanowicz, Boron-enhanced growth of micron-scale carbon-based nanowalls: a route toward high rates of electrochemical biosensing, *ACS Appl. Mater. Interface* 9 (2017) 12982–12992.
- J.-H. Zhong, J. Zhang, X. Jin, J.-Y. Liu, Q. Li, M.-H. Li, W. Cai, D.-Y. Wu, D. Zhan, B. Ren, Quantitative correlation between defect density and heterogeneous electron transfer rate of single layer graphene, *J. Am. Chem. Soc.* 136 (2014) 16609–16617.
- P. Hirunsit, M. Liangruksa, P. Khanchaitit, Electronic structures and quantum capacitance of monolayer and multilayer graphenes influenced by Al, B, N and P doping, and monovacancy: theoretical study, *Carbon* 108 (2016) 7–20.
- L. Ruitao, C. Tongxiang, J. Mun-Suk, Z. Qiang, C. Anyuan, S.D. Sheng, Z. Zhongjun, Y. Seong-Ho, M. Jin, M. Isao, K. Feiyu, Open-ended, N-doped carbon nanotube-graphene hybrid nanostructures as high-performance catalyst support, *Adv. Funct. Mater.* 21 (2011) 999–1006.
- A.M. Oliveira-Brett, L.A.d. Silva, C.M.A. Brett, Adsorption of guanine, guanosine, and adenine at electrodes studied by differential pulse voltammetry and electrochemical impedance, *Langmuir* 18 (2002) 2326–2330.
- C.M.A. Brett, A.M.O. Brett, *Electrochemistry: principles, methods, and applications*, Oxford Press, 1993.